IOPscience iopscience.iop.org

Home Search Collections Journals About Contact us My IOPscience

Ab initio calculations of cohesive and structural properties of the alkali-earth oxides

This article has been downloaded from IOPscience. Please scroll down to see the full text article.

1996 J. Phys.: Condens. Matter 8 8983

(http://iopscience.iop.org/0953-8984/8/46/005)

View the table of contents for this issue, or go to the journal homepage for more

Download details:
IP Address: 171.66.16.207
The article was downloaded on 14/05/2010 at 04:29

Please note that terms and conditions apply.

J. Phys.: Condens. Matter **8** (1996) 8983–8994. Printed in the UK

Ab initio calculations of cohesive and structural properties of the alkali-earth oxides

Pietro Cortona† and Andrea Villafiorita Monteleone‡

† Laboratoire de Structure Electronique et Modélisation des Milieux Condensés (SEM), Ecole Centrale Paris, Grande Voie des Vignes, 92295 Châtenay-Malabry Cedex, France

‡ Dipartimento di Fisica, Università di Modena, Via Campi 213a, I-41100 Modena, Italy

Received 15 May 1996, in final form 17 July 1996

Abstract. We have performed *ab initio* self-consistent calculations of the standard cohesive properties (equilibrium lattice parameters, binding energies and bulk moduli) of the four alkali-earth oxides (MgO, CaO, SrO and BaO) having the B1 (NaCl-like) phase under normal temperature and pressure conditions. We have also studied the relative stability of the B1 and B2 (CsCl-like) phases, and the behaviour, under pressure of these crystals (equations of state, transition pressures and changes of volume for the structural phase transition B1 → B2). All the calculations were performed in the framework of the density-functional theory by a method which allows the direct calculation of the ground-state electron density of a system without the preliminary determination of its wavefunctions and energy eigenvalues.

1. Introduction

The alkali-earth oxides are compounds which have technological applications ranging from catalysis to microelectronics. They are important constituents of the Earth's lower mantle and their properties under very high pressures have been studied intensively. Furthermore, they have served in the past as prototypical oxides for testing semi-empirical theories or *ab initio* calculations. Thus, a variety of theoretical and experimental studies of their properties is actually available in the literature.

Band-structure calculations for all the compounds considered in the present paper (MgO, CaO, SrO and BaO) have been performed by the linearized-augmented-plane-waves (LAPW) [1–3] and by the linear-muffin-tin-orbitals (LMTO) [4, 5] methods. Results for MgO and (in some cases) for CaO have also been obtained by using first-principles pseudo-potentials [6], the Korringa–Kohn–Rostoker (KKR) method [7] and the APW [8] method. With the exception of [3], in which the optical properties were considered, all these papers reported results for the cohesive properties and (in some cases) for the behaviour under pressure of these crystals. All these calculations were performed within the framework of the density-functional theory (DFT), using the local-density approximation (LDA) for the exchange and the correlation energies.

Hartree–Fock (HF) calculations, whether including corrections for the correlation contributions to the total energy or not, have been published for MgO, CaO and SrO [9–11]: in particular, Pandey *et al* [9] focused on the features of the band structure of these solids, whereas Dovesi *et al* [10] and Zupan *et al* [11] reported values for the cohesive properties and a study of SrO under pressure.

0953-8984/96/458983+12$19.50 © 1996 IOP Publishing Ltd

From the experimental point of view, the behaviour under pressure of these solids has been investigated by several authors. In particular, a transition from the B1 (NaCl-like) to the B2 (CsCl-like) phase was detected for CaO by Jeanloz *et al* [12] and by Mammone *et al* [13]; Sato and Jeanloz [14] observed a similar transition for SrO, whereas BaO has been found to have a first transition from the B1 phase to a tetragonal [15] or a hexagonal [16] phase at approximately 9 GPa and a second transition to a tetragonal PH_4I phase at 15 GPa [15, 16]. MgO is stable in the B1 phase at least until 200 GPa [17]; whether it undergoes a phase transition at a higher pressure (as predicted by the theory) is, to the best of our knowledge, still an open question.

The results reported in the present paper were obtained by using a DFT method [18] which allows the direct calculation of the electron density and of the total energy of a system; the preliminary determination of the energy eigenvalues is unnecessary. The method is based on the Hohenberg–Kohn variational principle [19], that requires a computational effort which increases approximately in a linear way with the size of the system and can be applied to periodic as well as to non-periodic systems.

In this paper, we consider the four alkali-earth oxides having the B1 structure under normal temperature and pressure conditions. Our objective is twofold: on the one hand, to perform a systematic study of the cohesive properties and of the behaviour under pressure of these crystals and on the other hand, to compare our results carefully with those of *ab initio* calculations and with the experimental data. This comparison will support the use of the method in the cases for which a similarly detailed analysis is impossible [20].

2. The method

The Hohenberg–Kohn theorems [19] state that the ground-state electron density of a system can be found by seeking the minimum of the total energy functional:

$$E_v[\rho] = T[\rho] + J[\rho] + E_{xc}[\rho] + \int V_{ext}(\boldsymbol{r})\rho(\boldsymbol{r})\,\mathrm{d}^3r\,. \tag{1}$$

In this equation $T[\rho]$ is the kinetic energy of a fictitious system of non-interacting electrons having the same density as the real system, $J[\rho]$ is the electrostatic energy, $E_{xc}[\rho]$ is the exchange-correlation energy and the last term gives the interaction energy associated with the external potential.

In an equivalent way, the ground-state electron density can be found by solving the Kohn–Sham equation [21]

$$\left(-\frac{1}{2}\nabla^2 + V_{ext}(\boldsymbol{r}) + \frac{\delta J}{\delta\rho} + \frac{\delta E_{xc}}{\delta\rho}\right)\psi_i(\boldsymbol{r}) = \varepsilon_i\psi_i(\boldsymbol{r}) \tag{2}$$

and then calculating the electron density by

$$\rho(\boldsymbol{r}) = \sum_i 2n_i|\psi_i(\boldsymbol{r})|^2\,. \tag{3}$$

The coefficients n_i take the values unity or zero for levels under or above the Fermi energy, respectively. They can take fractional values for levels coinciding with the Fermi one. The factor of 2 is due to the fact that we are implicitly considering the non-spin-polarized case.

In the Kohn–Sham method the electron density is obtained by means of intermediate quantities (the one-electron wavefunctions) which have no physical meaning in the context of the DFT. In the case of a crystal, a complete band-structure calculation has to be performed and the corresponding algorithms require a computational time which grows approximately as N^3, the cube of the number of valence electrons of the system.

In recent years, some methods have been proposed which allow the determination of the ground-state charge density directly from equation (1) or with a computational effort growing less rapidly than N^3 [18, 22–25]. In this paper we will use the method proposed by Cortona [18], which we describe briefly below.

Let us consider a non-magnetic crystal (or molecule) and partition it into sub-systems. This means that we have chosen some points within the primitive cell, and we have associated with each point some nuclear charges (zero, one or several) and one (unknown) electron density. The total electron density of the crystal is given by the superposition of the electron densities of the sub-systems:

$$\rho(\boldsymbol{r}) = \sum_{j,k} \rho_j(\boldsymbol{r} - \boldsymbol{R}_k - \boldsymbol{\tau}_j) = \sum_{j,k} \rho_{jk} \tag{4}$$

where $\boldsymbol{R}_k$ are the vectors of the Bravais lattice and $\boldsymbol{\tau}_j$ are the position vectors of the partition points within the primitive cell corresponding to $\boldsymbol{R}_k = \boldsymbol{0}$. The partial electron densities $\rho_{jk}(\boldsymbol{r})$ can be written (in a non-unique way) in terms of one-electron wavefunctions:

$$\rho_j(\boldsymbol{r} - \boldsymbol{R}_k - \boldsymbol{\tau}_j) = \sum_i 2n_{ij}|\psi_{ij}(\boldsymbol{r} - \boldsymbol{R}_k - \boldsymbol{\tau}_j)|^2 \tag{5}$$

and are supposed to be localized, in the sense that the ψ_{ij} are required to decrease exponentially when $|\boldsymbol{r} - \boldsymbol{R}_k - \boldsymbol{\tau}_j|$ tends to infinity. Note that the ψ_{ij} are not wavefunctions of the overall system; they are supposed to be normalized and, if they are centred on the same point $\boldsymbol{R}_k - \boldsymbol{\tau}_j$, orthogonal. The coefficients n_{ij} are fermionic occupation numbers ($0 \leqslant n_{ij} \leqslant 1$) and satisfy the condition

$$\sum_{ij} 2n_{ij} = \frac{N}{N_c} \tag{6}$$

where N is the total number of electrons and N_c is the number of primitive cells of the crystal. In contrast, no restriction is imposed in the sum on i: the result can be fractional.

For each choice of occupation numbers and wavefunctions producing a given $\rho_{jk}(\boldsymbol{r})$, we define a kinetic energy in the usual way:

$$T[n_{ij}, \psi_{ij}] = \sum_i 2n_{ij} \left\langle \psi_{ij} \left| -\tfrac{1}{2}\nabla^2 \right| \psi_{ij} \right\rangle. \tag{7}$$

We split the total kinetic energy of the system $T[\rho]$ into the sum of the 'internal' kinetic energies of the sub-systems and a contribution coming from the interaction of the sub-systems:

$$T[\rho] = \sum_{j,k} T[n_{ij}, \psi_{ij}] + \left(T[\rho] - \sum_{j,k} T[n_{ij}, \psi_{ij}] \right). \tag{8}$$

The internal terms are treated exactly, whereas an approximation is used for the inter-sub-systems kinetic energy.

Suppose that $T^a[\rho]$ and $E^a_{xc}[\rho]$ are approximate expressions for the kinetic energy and the exchange-correlation energy functionals. We replace the exact total energy functional with the following:

$$E^a[n_{ij}, \psi_{ij}] = \sum_{j,k} T[n_{ij}, \psi_{ij}] + \left(T^a[\rho] - \sum_{j,k} T^a[\rho_{jk}] \right) + J[\rho] + E^a_{xc}[\rho] + \int V_{ext}(\boldsymbol{r})\rho(\boldsymbol{r})\, \mathrm{d}^3\boldsymbol{r} \tag{9}$$

and we seek the minimum value of this functional by varying the wavefunctions ψ_{ij} and the occupation numbers n_{ij}.

By performing the variation, we find that the wavefunctions ψ_{ij} must satisfy the Kohn–Sham-like equation

$$\left(-\tfrac{1}{2}\nabla^2 + V_{eff}\right)\psi_{ij}(\boldsymbol{r} - \boldsymbol{R}_k - \boldsymbol{\tau}_j) = \varepsilon_{ij}\psi_{ij}(\boldsymbol{r} - \boldsymbol{R}_k - \boldsymbol{\tau}_j) \tag{10}$$

with

$$V_{eff} = V_{ext} + \frac{\delta J}{\delta \rho} + \frac{\delta E^a_{xc}}{\delta \rho} + \frac{\delta T^a}{\delta \rho} - \frac{\delta T^a}{\delta \rho_{jk}} \tag{11}$$

and that the occupation numbers, the total energy of the crystal and the energy eigenvalues are related by

$$\varepsilon_{ij} = \frac{1}{2N_c}\frac{\partial E^a}{\partial n_{ij}}\,. \tag{12}$$

Equation (10) is a set of equations (one for each orbital of each sub-system) which must be solved simultaneously and self-consistently. The partial charge densities are then determined by equation (5), with the occupation numbers chosen according to the Fermi statistics. All the interactions of the sub-systems are contained in the effective potential (equation (11)). This potential can be divided into a contribution internal to a given sub-system and a 'crystalline' potential. The latter can be split into a short-range contribution, which needs to be taken into account only up to a finite order of neighbours, and a long-range contribution, that can be summed up to all orders of neighbours by the Ewald technique. Further details on these latter points can be found in [26].

3. Technical remarks

In all the calculations we have used the local approximation for the inter-sub-systems kinetic energy, for the exchange and for the correlation energy. The latter was taken into account by using the Ceperley–Alder–Perdew–Zunger expression [27]. We chose partition points τ_j coinciding with the atomic positions and derived the effective potentials from spherically averaged electron densities around each site.

In order to determine the total energy curve, we performed a large set of self-consistent calculations for each compound. The lattice parameters (between 20 and 30, depending on the system) were taken equally spaced (0.05 and 0.03 Å for the B1 and the B2 structures, respectively) and approximately symmetrically disposed around the experimental one. Very severe self-consistency tests were imposed in order to guarantee a high level of numerical accuracy [28]. All the calculations were fully relativistic, in the sense that the Schrödinger-like equation (10) was replaced by the corresponding Dirac-like equation. The latter was solved numerically, by means of standard techniques [29, 30]. The radial integration mesh was chosen thick enough to reproduce correctly the rapid variations in the effective potential at the distances corresponding to the various orders of neighbours.

We fitted the total energy values by polynomials from second to sixth degree of the lattice parameter a as well as of $V^{-2/3}$ (Birch's equation; V is the volume of the primitive cell). The number of calculated points used in the best fits was reduced progressively in a symmetrical way around the predicted equilibrium lattice parameter. The values of the cohesive energies, the lattice parameters and the bulk moduli obtained from the total energies curves fitted by polynomials $P(a)$ of fourth, fifth and sixth degree were practically the same and were insensitive to the reduction in the number of points used in the best fit. The spread of the bulk modulus values for each crystal and for each phase was contained within (and very often was smaller than) 0.5 GPa around some mean value. The results reported in tables 3 and 8 (later) were obtained by rounding these mean values. No fluctuations at all

were noticed for the values of the equilibrium lattice parameters and of the cohesive energies. The results obtained by fitting the calculated values by means of the Birch equations of state $P(V^{-2/3})$ of various order were identical to the preceding ones within the precision shown in the tables.

As mentioned above, all our calculations were performed using effective potentials that are spherically symmetrical around the partition points $\boldsymbol{\tau}_j$. Thus, the partial electron densities ρ_{jk} are spherically symmetrical. However, the total electron density ρ resulting from the superposition of the ρ_{jk} (equation (4)) is non-spherical and the contributions due to its non-sphericity can be taken into account, or not, when the total energy is calculated. Both types of results will be reported in the following. In practice, in a 'non-spherical' calculation, the various contributions to the total energy per primitive cell were obtained by performing tridimensional integrals of the type

$$\int_{cell} \rho\varepsilon[\rho]\,\mathrm{d}^3r \tag{13}$$

where $\varepsilon[\rho]$ is the pertinent energy density. In a 'spherical' calculation, these integrals were rewritten as follows:

$$\int_{cell} \rho\varepsilon[\rho]\,\mathrm{d}^3r = \sum_{j,k}\int_{cell} \rho_{jk}\varepsilon[\rho]\,\mathrm{d}^3r = \sum_{j}\int_{all\ space} \rho_{j0}\varepsilon[\rho]\,\mathrm{d}^3r \tag{14}$$

and then the total electron density ρ was replaced by its spherical average around the point $\boldsymbol{\tau}_j$ [31]. This second procedure is consistent with the use of effective potentials derived from spherically averaged electron densities and the results obtained in such a way are completely self-consistent. In the first procedure, the non-spherical contributions are taken into account at the level of accuracy of first-order perturbation theory.

4. Results and comments

In tables 1–4 are reported our results for the cohesive properties of the alkali-earth oxides as well as the corresponding experimental data and the results of LAPW [1, 2], LMTO [4, 5], KKR [7] and HF [10, 11] calculations. All the experimental data refer to room-temperature conditions, whereas the theoretical values are pertinent to the static crystal. Thermal corrections should be introduced in order to perform a consistent comparison. In the cases of MgO and CaO these corrections have been evaluated by Mehl *et al* [1]: they are practically negligible for the lattice parameters and the binding energies, while the bulk moduli should be increased by 7–8 GPa.

Table 1. Calculated and experimental lattice parameters in ångström units.

	Experimental[a]	Non-spherical[b]	Spherical[b]	LAPW[c]	LMTO[d]	KKR[e]	HF[f]
MgO	4.21	4.20	4.27	4.17	4.09	4.22	4.20
CaO	4.81	4.76	4.84	4.72	4.65	4.82	4.87
SrO	5.16	5.10	5.18	5.07	5.22		5.23
BaO	5.54	5.43	5.52	5.44	5.51		

[a] Experimental results [32].
[b] 'Non-spherical' and 'spherical' calculations (present work, see text).
[c] Full-potential linearized augmented plane waves [1, 2].
[d] Linear muffin-tin orbitals [4, 5].
[e] Korringa–Kohn–Rostoker [7].
[f] LCAO Hartree–Fock [10, 11].

Table 2. Calculated and experimental binding energies (referred to free atoms) in electron-volts.

	Experimental[a]	Non-spherical[b]	Spherical[b]	LMTO[b]	KKR[b]	HF[b]
MgO	10.3	10.5	9.7	10.7	11.6	7.3
CaO	11.0	11.8	11.2	9.1	12.5	7.6
SrO	10.4	10.9	10.5	9.8		6.6
BaO		11.0	10.6	12.4		

[a] [33].
[b] As in table 1.

Table 3. Calculated and experimental bulk moduli in gigapascals. The values marked by an asterisk were determined at the experimental lattice parameters, whereas all the other theoretical values correspond to the calculated equilibrium lattice parameters.

	Experimental[a]	Non-spherical[b]	Spherical[b]	LAPW[b]	LMTO[b]	KKR[b]	HF[b]
MgO	160	163	150	170	171*	171	186
CaO	111	111	103	129	96	119	128
SrO	89	88	82	106	107*		108
BaO	74	73	68	86	70		

[a] [34, 35].
[a] As in table 1.

Table 4. Relative stability of the B1 and B2 phases at zero pressure, $E(\mathrm{B2}) - E(\mathrm{B1})$ in rydbergs.

	Non-spherical[a]	Spherical[a]	LAPW[a]
MgO	0.124	0.108	0.111
CaO	0.089	0.077	0.065
SrO	0.069	0.061	0.051
BaO	0.065	0.059	0.033

[a] As in table 1.

When considering the various theoretical results reported in the tables, it should be taken into account that the LAPW calculations include the non-spherical contributions to the total energy, thus they shall be compared with our non-spherical results. On the other hand, our spherical results shall be compared with those obtained by LMTO or KKR calculations. Looking at the results of these two latter methods, it is easy to note that the discrepancies are quite large. Because in both calculations the LDA was used and spherical averaging of the potential was performed, these discrepancies can only be attributed to the different way of solving the band-structure problem.

In table 1, it can be seen that our calculated lattice parameters agree with the experimental results to within 2% and with the LAPW ones to within 1%. The agreement is also excellent between our spherical calculations and the KKR ones, whereas greater discrepancies are found with respect to LMTO calculations.

Our calculated binding energies (table 2) compare well with the experimental data. In particular, we correctly find the greatest binding energy for CaO and similar values for MgO and SrO. This trend is not correctly reproduced by the LMTO method.

The calculated bulk moduli are compared with the experimental data in table 3. Precise measurements of the bulk moduli are quite difficult: the values reported in table 3 are due to Chang and Barsch [34] and Chang and Graham [35], who measured the elastic constants

of these crystals by ultrasonic techniques. These values agree within a few gigapascals with the results of similar measurements performed by Marklund and Mahmoud [36] and by Son and Bartels [37]. Our non-spherical bulk moduli are in excellent agreement with the experimental data at room temperature. However, as we have already pointed out, the latter should be extrapolated to the static crystal. The resulting values will be between our results and the LAPW ones.

The relative stability of the B1 and B2 phases is studied in table 4. It can be seen that all these compounds are stable in the B1 phase at $p = 0$, in agreement with experiment.

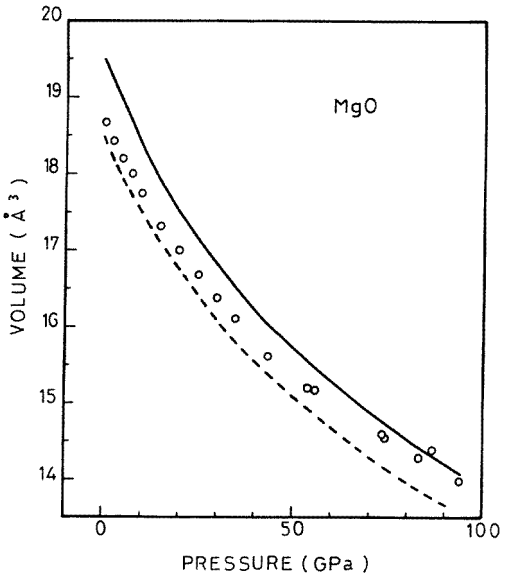

Figure 1. The equation of state for MgO. The full and broken curves correspond to our spherical and non-spherical calculations, respectively. The experimental data (circles) were taken from [38, 39].

Table 5. Calculated and experimental pressures in gigapascals for the transition from the B1 to the B2 phase.

	Experimental	Non-spherical[a]	Spherical[a]	LAPW[a]	APW[b]	Psuedo-potential[c]
MgO	> 200[d]	370	227	518	205	1050
CaO	63[e]	122	75	56	32	
SrO	36[f]	63	42	29		

[a] As in table 1.
[b] Augmented plane waves [8].
[c] First-principles pseudo-potentials [6].
[d] [17].
[e] [13].
[f] [14].

In tables 5 and 6, and in figures 1–3, the behaviour under pressure and the phase transition from the B1 phase to the B2 one are investigated. Figures 1–3 show that the behaviour under pressure of these crystals is quite accurately reproduced. In particular, for

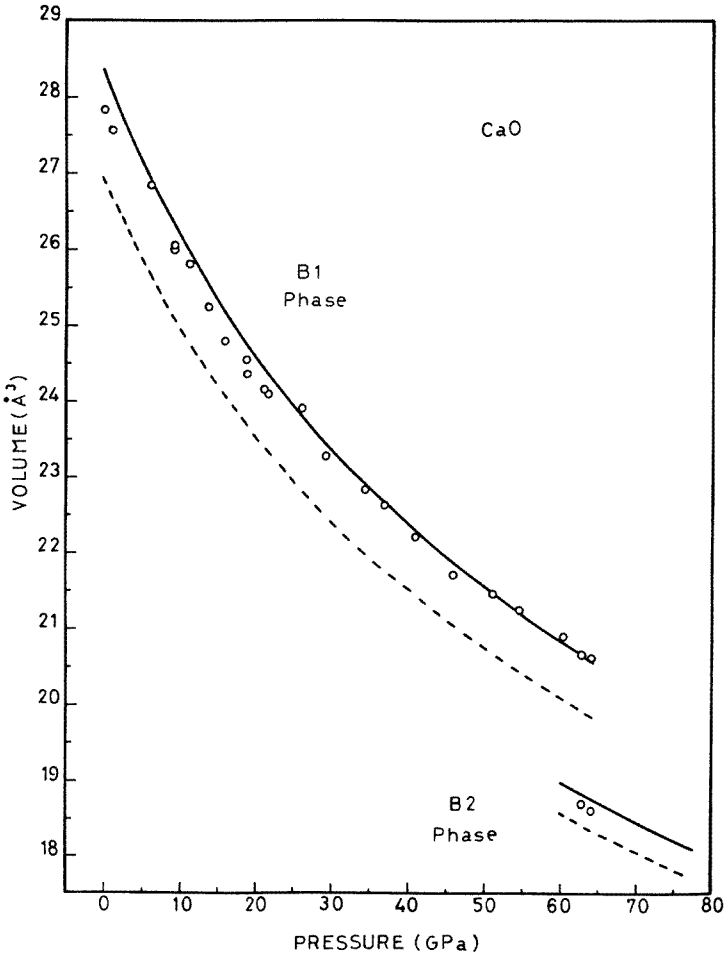

Figure 2. The equation of state for CaO. The full and broken curves correspond to our spherical and non-spherical calculations, respectively. The experimental data (circles) were taken from [13].

Table 6. Percentage changes in volume $(V(\mathrm{B1}) - V(\mathrm{B2}))/V(\mathrm{B1}) \times 100$ at the phase transition.

	Experimental	Non-spherical[a]	Spherical[a]	LAPW[a]	Pseudo-potential[b]
MgO		5.8	7.1	4.7	4.8
CaO	9.7[c]	7.0	9.0	11	
SrO	12[d]	7.8	9.8	12	

[a] As in table 1.
[b] As in table 5.
[c] [13].
[d] [14].

CaO and SrO the spherical results generally agree with the experimental data within the experimental errors. The non-spherical results tend to underestimate the pressure required to obtain a given volume: this reflects the fact that the equilibrium lattice parameter at

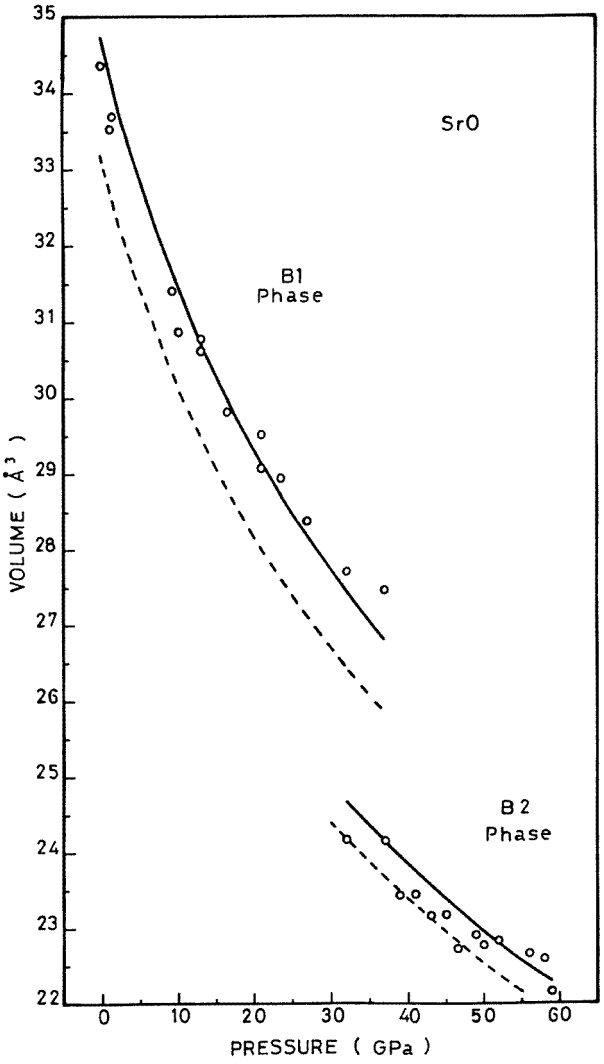

Figure 3. The equation of state for SrO. The full and broken curves correspond to our spherical and non-spherical calculations, respectively. The experimental data (circles) were taken from [14].

$p = 0$ is slightly underestimated. It can be seen that the discrepancies between calculated and experimental volumes at high pressures are similar to the discrepancies at $p = 0$. This means that, in the overall range of pressures considered, the discrepancies in the lattice parameters are of a few per cent. Similar considerations also apply to MgO, with the additional remarks that in this case the slope of the $p(V)$ curve is less well reproduced and that the experimental data agree almost equally well with the non-spherical and the spherical results. In table 5 are reported the calculated and experimental transition pressures from the B1 to the B2 phases and in table 6 the corresponding changes in volume. It can be seen that the non-spherical results overestimate the transition pressures for CaO and SrO by about a factor of two, whereas the spherical results are in much better agreement with the

Table 7. Calculated lattice parameters for the B2 phase in ångström units.

	Non-spherical[a]	Spherical[a]	LAPW[a]
MgO	2.59	2.62	2.60
CaO	2.90	2.93	2.85
SrO	3.10	3.13	3.04
BaO	3.31	3.34	3.24

[a] As in table 1.

Table 8. Calculated bulk moduli for the B2 phase in gigapascals.

	Non-spherical[a]	Spherical[a]	LAPW[a]
MgO	163	155	170
CaO	119	113	129
SrO	99	94	106
BaO	84	79	86

[a] As in table 1.

experiments, the discrepancies being similar to those of the LAPW results.

Finally, in table 7 and 8 are reported the equilibrium lattice parameters and bulk moduli for the B2 phase. Certainly, these quantities cannot be measured experimentally. Nevertheless, knowledge of them is required in order to write some analytical equations of state. The values that we have obtained are in good agreement with the LAPW ones.

5. Conclusions

The results reported in this paper show that the method we have used gives an accurate description of the cohesive properties of the alkali-earth oxides. All these crystals are found to be stable in the experimentally correct crystallographic phase and their equation of state is quite accurately reproduced. However, the results for the transition pressures of CaO and SrO are not satisfactory: we obtain good results by the spherical calculations, but not by the non-spherical ones, which are, in principle, the more accurate ones. It is worth noticing that, in the case of the alkali-earth sulphides [20], we found transition pressures in reasonable agreement with experiment. Thus, in order to establish whether the discrepancies between the calculated values and the experimental data have some well defined trend, further calculations on other ionic systems are needed.

The comparison with the band-structure calculations indicates that our results are about as accurate as those obtained by the very sophisticated full-potential LAPW method and more accurate than the results obtained by a method such as the LMTO one, which uses the atomic sphere approximation. In any case, at least for the systems considered in this paper, the additional approximation on the kinetic energy which characterizes the method has only minor consequences: our results are well within the spread of values produced by the different techniques and approximations used in the band-structure calculations for solving the Kohn–Sham equation.

The main advantages of the method are its simplicity, that there is a linear increase in computing time with the size of the system and the non-crucial role of the crystal periodicity. It is precisely this last feature of the method which promises to be particularly useful for studying partially disordered solids. However, in order to take advantage of these features of

the method completely, a more complete inclusion of the non-spherical effects is required: the present version of our program cannot correctly treat systems whose electron density is far from a superposition of spherical densities. More generally, it cannot give a good account of the properties that are strongly affected by the non-sphericity of the sub-system electron densities. Thus, it is important to notice that the spherical approximation is not an intrinsic feature of the method and that it can be removed in future calculations. We believe that our method can be usefully applied to the study of molecular crystals: the good agreement with experimental data of the results for the rare-gas crystals [40] is a strong indication in that direction. For general molecular systems, the natural partition units are the molecules and equation (10) must be solved by using a molecular-like program, with the non-spherical contributions included in the effective potential. Finally, we notice that a way of including the non-spherical contributions in the calculations self-consistently, consists of solving equation (10) by diagonalizing the Hamiltonian on a localized basis set. This approach, which has been used successfully by Yang [22, 41] in the context of a similar theory, can be particularly useful for covalent systems, such as, for example, typical semiconductors.

Acknowledgment

We would like to thank M J Mehl for giving us his unpublished LAPW results and for useful discussions.

References

[1] Mehl M J, Cohen R E and Krakauer H 1988 *J. Geophys. Res.* **93** 8009; 1989 *J. Geophys. Res.* **94** 1977
[2] Mehl M J Private communication
[3] Stepanyuk V S, Szász A, Grigorenko A A, Katsnelson A A, Farberovich O V, Mikhalin V V and Hendry A 1992 *Phys. Status Solidi* b **173** 633
[4] Taurian O E, Springborg M and Christensen N E 1985 *Solid. State. Commun.* **55** 351
[5] Springborg M and Taurian O E 1986 *J. Phys. C.: Solid State Phys.* **19** 6347
[6] Chang K J and Cohen M L 1984 *Phys. Rev.* B **30** 4774
[7] Yamashita J and Asano S 1983 *J. Phys. Soc. Japan* **52** 3506
[8] Bukowinski M S T 1985 *Geophys. Res. Lett.* **12** 536
[9] Pandey R, Jaffe J E and Kunz A B 1991 *Phys. Rev.* B **43** 9228
[10] Dovesi R, Roetti C, Freyria-Fava C, Aprà E, Saunders V R and Harrison N M 1992 *Phil. Trans. R. Soc.* A **341** 203
[11] Zupan A, Petek I, Causà M and Dovesi R 1993 *Phys. Rev.* B **48** 799
[12] Jeanloz R, Ahrens T J, Mao H K and Bell P M 1979 *Science* **206** 829
[13] Mammone J P, Mao H K and Bell P M 1981 *Geophys. Res. Lett.* **8** 140
[14] Sato Y and Jeanloz R 1981 *J. Geophys. Res.* **86** 11 773
[15] Liu L and Bassett W A 1972 *J. Geophys. Res.* **77** 4934
[16] Weir S T, Vohra Y K and Ruoff A L 1986 *Phys. Rev.* B **33** 4221
[17] Vassiliou M S and Ahrens T J 1981 *Geophys. Res. Lett.* **8** 729
[18] Cortona P 1991 *Phys. Rev.* B **44** 8454
[19] Hohenberg P and Kohn W 1964 *Phys. Rev.* **136** B864
[20] This is the case, for example, for the alkali-earth sulphides. Cortona P, Villafiorita Monteleone A and Becker P 1995 *Int. J. Quantum Chem.* **56** 831
[21] Kohn W and Sham L J 1965 *Phys. Rev.* **140** A1133
[22] Yang W 1991 *Phys. Rev. Lett.* **66** 1438
[23] Baroni S and Giannozzi P 1992 *Europhys. Lett.* **17** 547
[24] Galli G and Parrinello M 1992 *Phys. Rev. Lett.* **69** 3547
[25] Kohn W 1993 *Chem. Phys. Lett.* **208** 167
[26] Cortona P 1992 *Phys. Rev.* B **46** 2008

[27] Perdew J P and Zunger A 1981 *Phys. Rev.* B **23** 5048
[28] We have assumed to have found the self-consistent solution of equation (10) once the following conditions have been verified simultaneously: (i) relative errors in the energy eigenvalues smaller than 10^{-9}; (ii) relative or absolute errors in the wavefunctions smaller than 0.5×10^{-8} and (iii) relative or absolute errors on the effective potential smaller than 0.5×10^{-8}. Using these convergence tests, the spherical calculation of the overall total energy curve (25 lattice parameters) for MgO in the B1 phase takes 21 min on a 3CT IBM workstation.
[29] Grant I P 1970 *Adv. Phys.* **19** 747
[30] Desclaux J P, Mayers D F and O'Brien F 1971 *J. Phys. B: At. Mol. Phys.* **4** 631
[31] For example, the inter-sub-systems kinetic energy per primitive cell is given by
$$\tfrac{3}{10}(3\pi^2)^{2/3}\int_{cell}\left(\rho^{5/3}-\sum_{jk}\rho_{jk}^{5/3}\right)\mathrm{d}^3r$$
in non-spherical calculations and by
$$\tfrac{3}{10}(3\pi^2)^{2/3}\sum_{j}\int_{all\ space}\rho_{j0}\left(\langle\rho\rangle_j^{2/3}-\rho_{j0}^{2/3}\right)\mathrm{d}^3r$$
in spherical calculations ($\langle\cdot\rangle_j$ indicates the spherical average around $\boldsymbol{\tau}_j$).
[32] Madelung O (ed) 1982 *Numerical Data and Functional Relationships in Science and Technology* Landolt-Börnstein, Group III, vol 17, part b (New York: Springer)
[33] Wagman D D, Evans W H, Parker V B, Schumm R H, Bailey S M, Halow I, Churney K L and Nuttall R L 1990 *Handbook of Chemistry and Physics (1989–1990)* 70th edn, ed R C Weast (Boca Raton, FL: Chemical Rubber Company)
[34] Chang Z P and Barsch G R 1969 *J. Geophys. Res.* **74** 3291
[35] Chang Z P and Graham E K 1977 *J. Phys. Chem. Solids* **38** 1355
[36] Marklund K and Mahmoud S A 1971 *Phys. Scr.* **3** 75
[37] Son P R and Bartels R A 1972 *J. Phys. Chem. Solids* **33** 819
[38] Perez-Albuerne E A and Drickamer H G 1965 *J. Chem. Phys.* **43** 1381
[39] Mao H K and Bell P M 1979 *J. Geophys. Res.* **84** 4533
[40] Villafiorita Monteleone A 1993 *Laurea Thesis* Genoa
[41] Yang W 1991 *Phys. Rev.* A **44** 7823